ELSEVIER

Journal of Nuclear Materials 302 (2002) 211–216

journal of nuclear materials

www.elsevier.com/locate/jnucmat

Fatigue behavior of 20% cold-worked 316 stainless steel under in situ irradiation with 17 MeV protons at 60 °C

Y. Murase [a,*], Johsei Nagakawa [a,b], N. Yamamoto [a]

[a] *Materials Engineering Laboratory, National Institute for Materials Science, 1-2-1 Sengen, Tsukuba-shi, Ibaraki-ken 305-0047, Japan*
[b] *Interdisciplinary Graduate School of Engineering Sciences, Kyushu University, 6-1 Kasuga Koen, Kasuga, Fukuoka 816-8580, Japan*

Received 18 June 2001; accepted 12 January 2002

Abstract

Load-controlled fatigue tests in the mode of tension–tension were performed for the side-notched 20% cold-worked 316 stainless steel under in situ irradiation and following irradiation with 17 MeV protons at 60 °C. In comparison with the unirradiation tests, fatigue life was substantially prolonged for in situ irradiation tests, while a slight increase of fatigue life was detected in post-irradiation condition. The SEM measurements of spacing of fatigue striations on fracture surface suggested higher resistance to fatigue fracture in the in situ irradiation specimens. Some essential differences in the irradiation effects between in situ and post-irradiation conditions were summarized in this paper.

1. Introduction

The first wall of a fusion reactor will receive severe atomic displacement damage and thermal stress simultaneously. Since thermal stress was induced cyclically by periodic operations of fusion reactor, it is important to understand the material fatigue behavior under in situ irradiation in order to evaluate its feasibility for fusion reactor application. Although a number of studies have been focused on the irradiation effect on fatigue behavior, most works have dealt with the fatigue response in the post-irradiation condition [1–4]. In this case, the radiation-induced defect clusters were already introduced to the specimen prior to the cyclic loading and the in situ (dynamic) irradiation effects on fatigue behavior could not be reflected in the experimental results. In the recent decades, several workers [5–7] have suggested some differences in fatigue behavior between in situ and post-irradiation conditions; a longer fatigue life in in situ irradiation tests than that in post-irradiation tests. However in these works, the mechanism of higher resistance to fracture in the in situ irradiation condition has not been clarified in the light of the in situ (dynamic) irradiation effect on fatigue processes such as crack initiation and propagation.

In the present study, stress-controlled fatigue tests in tension–tension mode were carried out for 20% cold-worked 316 stainless steel under in situ irradiation with 17 MeV protons at 60 °C. Post-irradiation and unirradiation fatigue tests were also conducted at the same condition. After the fatigue tests, fatigue striations on the fracture surface were examined by scanning electron microscope (SEM) for all the specimens. Tensile tests were also performed for the irradiated specimens in order to evaluate the changes in tensile stresses caused by atomic displacement damage. The objective of the present study is to investigate the in situ (dynamic) irradiation effect on fatigue behavior on the basis of the striation analysis for all the specimens.

2. Experimental procedure

The material used for the present study was a commercial 316 stainless steel. The chemical composition of

* Corresponding author. Tel.: +81-298 59 2838; fax: +81-298 59 2014.
E-mail address: murase.yoshiharu@nims.go.jp (Y. Murase).

0022-3115/02/$ - see front matter
PII: S0022-3115(02)00774-2

Table 1
Chemical compositions of 316 stainless steel (wt%)

C	Ni	Cr	Mn	Mo	Si	P	S	Fe
0.06	10.30	16.79	1.17	2.16	0.68	0.027	0.001	Balance

the alloy is given in Table 1. The cold-worked sheet of 0.15 mm in thickness was punched out into the specimen type shown in Fig. 1. The grain size was controlled to be less than 10 μm in order to keep the mechanical properties equivalent to that of truly polycrystalline materials [8]. A fatigue starter side-notch was introduced into the gauge of specimen by means of spark erosion as presented in Fig. 1. The notch was 0.60 mm in length and 0.12 mm wide with an end radius of 0.06 mm. Cyclic loading mode was tension–tension in load control with the maximum stress of 536.4 MPa and the minimum stress of 236.4 MPa under a constant loading rate of 50 MPa/s. The maximum stress is corresponding to 90% of yield stress at the notched ligament at 60 °C. In the present 17 MeV proton irradiation, atomic displacement rate was adjusted to 1×10^{-7} dpa/s with an error range of ±11%. As for the post-irradiation test, the specimen was pre-irradiated at the same dose level as integrated during the in situ irradiation test. The irradiation temperature was controlled at 60 °C by adjusting the flow rate of helium gas jet to compensate the beam heating under irradiation. In case of the post-irradiation and unirradiated tests, the heated helium jet was used to maintain the specimen temperature at 60 °C. The specimen temperature was monitored by two pairs of thermocouples attached directly to the gauge by spot welding. The two attaching points were upper and lower away from the expected crack propagation path by 2 mm, so that the spot welding would not affect the fatigue process. The maximum fluctuation of specimen temperature was 3 °C in the feedback system where the output of electric heater was successively adjusted by the reference signal of specimen temperature. Experimental details of specimen preparation, irradiation condition and the in-beam fatigue testing machine were described elsewhere [9]. After the fatigue tests, the morphology on fracture surface was examined by a SEM (JSM-5310) for all the specimens. Tensile tests were also performed for the irradiated specimens without a side-notch. Pre-irradiation dose levels were 0.0075, 0.0093 and 0.0143 dpa. The changes in tensile stresses were measured at each atomic displacement damage.

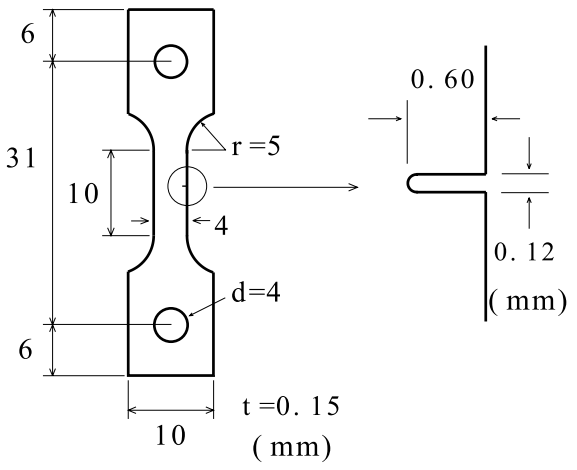

Fig. 1. Geometry of specimen for fatigue tests.

3. Results

3.1. Experimental data

The relative displacement of specimen at the maximum stress (536.4 MPa) was plotted against the number of cycles for in situ irradiation, post-irradiation and unirradiation fatigue tests, as shown in Fig. 2. The relative displacement is the difference of actual displacement at the maximum stress between the Nth cycle and the first cycle. The number of cycles to fracture (N_f) was 12050 and 10364 for in situ irradiation tests, and the total amount of dose level during irradiation was corresponding to 0.015 and 0.012 dpa, respectively. The higher atomic displacement of 0.015 dpa was adopted for the pre-irradiation dose level of the post-irradiation specimens. Fatigue life under in situ irradiation was prolonged by almost two times as that of unirradiation tests, while the extension of fatigue life was not so much for post-irradiation condition (see Fig. 2). Table 2 shows the changes in tensile stresses with increasing atomic displacement damage. The increase in ultimate tensile stress (UTS) and 0.2% offset yield stress (0.2% YS) at the dose level of 0.015 dpa was estimated to be about 70 and 200 MPa, respectively, indicating that the pre-irradiation induced irradiation hardening in the post-irradiation specimen.

Fig. 3 shows SEM photographs of fracture surfaces for (a) in situ, (b) post-irradiation and (c) unirradiated specimens at the distance of 550 μm from the notch tip. The SEM observation of the fracture surface revealed the existence of fatigue striations in the area from the notch tip to the ductile fracture region for all the specimens. Fig. 4 presents the plotting of striation spacing as a function of the distance from the notch tip for each specimen. Since striation spacing was too small to be

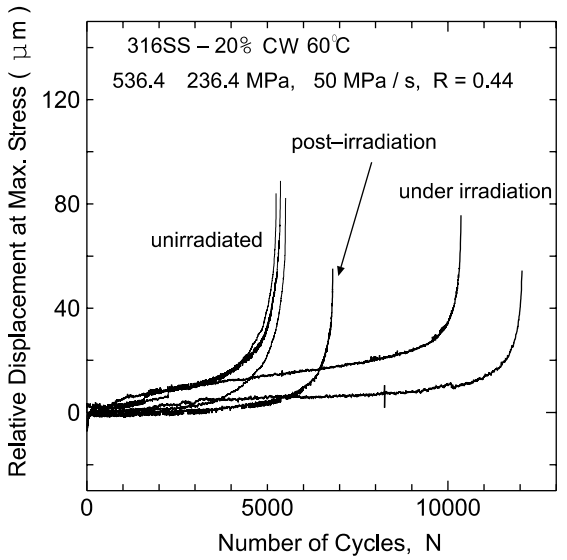

Fig. 2. Dependence of relative displacement on the number of cycles for each specimen.

Table 2
The changes in tensile stresses with increasing displacement damage

Dpa	UTS (MPa)	0.2% YS (MPa)
0	871	686
0.0075	887	831
0.0093	911	861
0.0143	945	882

resolved by SEM in the vicinity of the notch tip, the measurement was conducted in the area between the distance of 100 μm from the notch tip and the ductile fracture point. This area is designated as the striation area in the present paper. Striation spacing increased continuously with the distance from the notch tip for the unirradiated specimens, while the increase was less significant until 500 μm for both in situ and post-irradiation specimens. Although a steep increase of striation spacing was observed at 500 μm for post-irradiation specimen, a gradual increase over a more extended distance was detected in the in situ irradiation specimens. Fatigue crack has grown to 600–700 μm in length prior to the ductile fracture in both post-irradiation and unirradiated specimens, and it has grown to 800–900 μm in the in situ irradiation specimens.

3.2. Striation analysis

The relationship between fatigue cycles and striations has been investigated for many materials. Yokobori and Aizawa [10] have examined the application of one-to-one correlation for a 304 stainless steel in the range of temperature from 24 to 700 °C. The striation spacing was in good agreement with crack growth per one fatigue cycle when it was ranging from 0.1 to 1.0 μm at 24 °C [10]. Since the plots of striation spacing in the striation area were within this range for all specimens

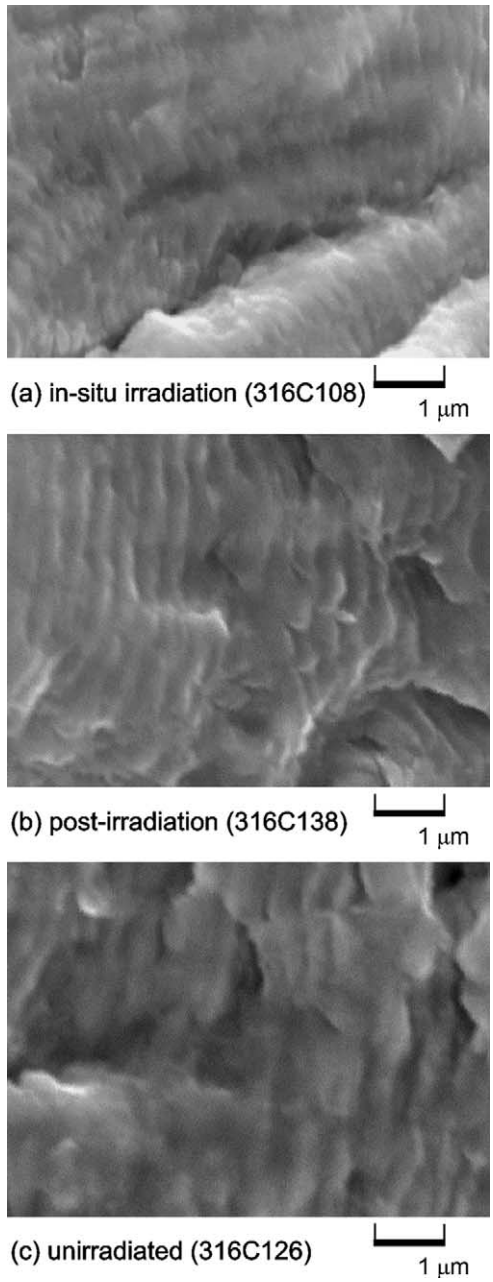

Fig. 3. Typical fracture surfaces of (a) in situ irradiation, (b) post-irradiation and (c) unirradiated specimens at the distance of 550 μm from the notch tip.

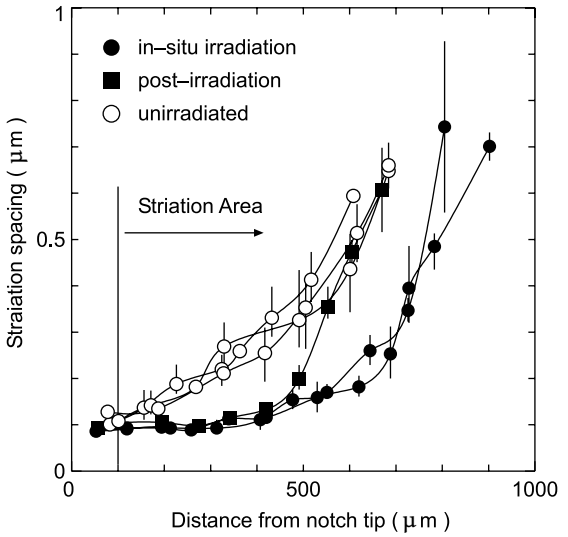

Fig. 4. The variation of striation spacing with increasing distance from notch tip.

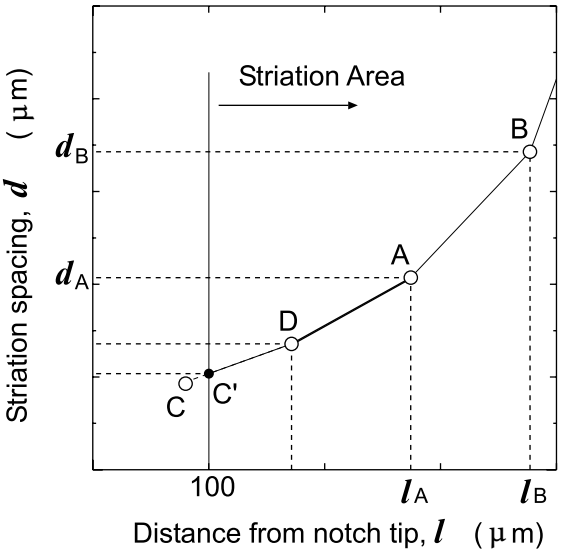

Fig. 5. Schematic plots of striation spacing versus distance from the notch tip.

(see Fig. 4), it seems to be reasonable to apply one-to-one correlation in the present results.

A statistical method to estimate the number of striations has been introduced by Connors [11]. Fig. 5 shows the schematic plots of striation spacing versus distance from the notch tip. The number of striation between two adjacent plots of A and B is given by the following equation:

Table 3
Comparison of the number of cycles for each stage of fatigue process in each irradiation condition

Sample name	Condition	N_f	N_c	N_i
316C58	In situ irradiation	10364	5301	5063
316C108	In situ irradiation	12050	5035	7015
316C138	Post-irradiaiton	6812	3859	2953
316C74	Unirradiation	5243	2437	2806
316C126	Unirradiation	5362	2183	3179
316C136	Unirradiation	5510	2522	2988

$$N_{A\to B} = \left[\frac{\ln d_B - \ln d_A}{(d_B - d_A)/(l_B - l_A)}\right], \quad (1)$$

where $d_{A,B}$ is the striation spacing and $l_{A,B}$ is the distance from the notch tip at the plot of A and B, respectively. When the plot of C is out of the striation area, the point of C′ on the line segment of C–D at 100 μm is used to calculate the number of striations in the line segment of C′–D. In the present measurements shown in Fig. 4, the sum of the number of striations in each segment for a specimen amounts to the total number of striations in the striation area (N_c). The calculated N_c represents the number of cycles to crack propagation from 100 μm until ductile fracture. The difference between N_f and N_c, which is denoted as N_i, corresponds to the number of cycles for crack initiation and growth until 100 μm in length. Table 3 presents N_f, N_c and N_i for each specimen. The increase in N_c was more pronounced in the in situ irradiation specimens than that in the post-irradiation specimen. Although N_i was similar for post-irradiation and unirradiated specimens, the increase in N_i was detected for the in situ irradiation specimens.

4. Discussion

It is well recognized that fatigue behaviors are closely associated with the development of dislocation structures. Evolution of dislocation structures during cyclic deformation was studied for a 316L type stainless steel at 20 °C [12]. The dislocation structures observed in the specimens were classified as tangles, cells and intermediate configurations (wall-channels, labyrinths and ladder-like structures). In general, these structures were formed in the first cycle, and the proportion of cells increased with cycling while that of tangles decreased constantly. The proportion of intermediate configurations increased at the early stage of cycling and then decreased slowly with cycling. It has been demonstrated that the rearrangement of dislocations from tangles into intermediate configurations is responsible for the cyclic softening. With further cycling, the intermediate configurations were gradually transformed to cell structures. The boundaries of cells were condensed with disloca-

tions and the interior of cells contained fewer dislocations in the saturation stage [12]. The cell structures were also reported in the plastic strain zone at the crack tip of a 316L type stainless steel at 25 °C [13] and even at elevated temperatures [14]. Some workers [15,16] have discussed the relationship between fatigue crack growth threshold and dislocation structure after numerous fatigue cycles. Since mobile dislocations induced by external cyclic loading were piled up at the cell walls, the back stress at the cell walls would become higher with cycling. At the critical condition, the intensity of back stress reached to a level sufficient to break down the stable cell structure. Therefore, the cell structure was considered as one of the intrinsic toughness factors that influence the fatigue crack growth threshold [15].

The effect of irradiation on material response has been discussed for 316 type stainless steels on the basis of the interaction between radiation-induced defects and dislocation structures [5,17–19]. The general assumption is that the radiation-induced defect clusters act as obstacles against the glide process of dislocations. The radiation-induced defect clusters cause an increase in yield strength and consequently a reduction in total elongation of the irradiated specimen. The increase in yield strength after irradiation was well correlated with the contribution of the radiation-induced defect clusters in AISI 316 stainless steel [18]. Although the radiation-induced defect clusters significantly modify the tensile properties, the density of these clusters would decrease during fatigue cycling. The microstructure evolution during cyclic loading was examined for 316 stainless steel irradiated with 200 keV Fe to a dose of 1×10^{16} ions/cm^2 at room temperature [19]. The formation of the dislocation-free wall-channels indicated that the moving glide dislocations produced by fatigue cycling would locally annihilate the radiation-induced defect clusters. Scholz [5] has reported fatigue response of 20% cold-worked 316L type stainless steel during strain-controlled cyclic loading under both in situ and post-irradiation with 19 MeV deuterons at 400 °C. Total elastic strain decreased during irradiation, while the fatigue loading after terminating the irradiation gave rise to a rapid softening of the material in a few cycles. The cyclic softening after the irradiation was resulted from a reduction of the density of the radiation-induced defect clusters. Although fatigue life was extended even in the post-irradiation condition, the increase of lifetime for the post-irradiation fatigue tests was not so much as that for the in situ irradiation tests [5]. Longer fatigue life under in situ irradiation was also reported for 316 stainless steel at 60 °C [6,7].

In the present study, the effect of irradiation on fatigue life was similar with the results demonstrated in some works [5–7]. The prolongation of fatigue life under in situ irradiation was more substantial than that of post-irradiation condition, as shown in Fig. 2. Table 3 shows that a substantial prolongation of fatigue life under in situ irradiation is attributed to the increase in number of cycles for crack initiation and growth until 100 μm in length (N_i) as well as the increase in number of cycles to propagation (N_c). Since the radiation-induced defect clusters are continuously introduced into the specimen under in situ irradiation, the density of defect clusters must be higher even in the intrinsic dislocation-free regions such as the wall-channel and the interior of well-developed cell structure. The higher density of defect clusters may enhance the arrest of dislocations and delay the pile-up of dislocations at the cell walls. The delayed achievement of the threshold stress to produce micro-cracks at the cell walls would contribute to the increase in both N_i and N_c in the in situ irradiation condition. As for the post-irradiation test, however, N_i was similar with that of unirradiation tests, as presented in Table 3. The increase in ultimate stress and yield stress shown in Table 2 appears to be little influential on N_i in the post-irradiation condition. Although a number of defect clusters are introduced into the material prior to the cyclic loading, the density of defect clusters would be quickly reduced due to local annihilation especially at the notch tip where plastic deformation is accumulated during cycling. Since numerous number of fatigue cycles are necessary to initiate cracks through the rearrangement of dislocation structures, a rapid decrease of the radiation-induced defect clusters at the notch tip may have little influence on N_i. At the process of crack propagation, a slight increase of N_c (see Table 3) was attributed to a lower growth rate of fatigue crack until 500 μm (see Fig. 2) in the post-irradiation condition. The radiation-induced defect clusters would survive and play some role in decreasing crack growth rate at the crack tip when the crack propagates at a moderate rate. Thus, the interaction of the radiation-induced defect clusters with moving dislocations appears to be one of the key mechanisms to understand the irradiation effect on fatigue behavior in both the in situ and post-irradiation conditions. The higher density of defect clusters during the in situ fatigue tests would explain the difference in the irradiation effect on fatigue behavior between in situ and post-irradiation conditions. It is noted that the higher resistance to fatigue fracture in the in situ irradiation condition was mainly responsible for the delay in the processes of crack initiation and growth until 100 μm in length.

The present results shown in Table 3 include inevitable errors due to the inherent scatter of fatigue lifetime. The striation spacing analysis used in this study is considered to be effective when the error range is within 10% [11]. In spite of possible errors originating from various resources, some essential differences in the effect of irradiation on fatigue behavior between in situ irradiation and post-irradiation conditions were demonstrated in the present experiments. More extensive

study on dislocation structures during in situ cycling is definitely needed to interpret the in situ fatigue behavior especially at higher temperatures where precipitates and voids are formed in the material.

5. Conclusion

Fatigue response of 20% cold-worked 316 stainless steel was examined under in situ irradiation and post-irradiation with 17 MeV protons at 60 °C. The lifetime of fatigue was substantially prolonged in the in situ irradiation condition, while a slight increase of lifetime was detected in the post-irradiation condition. The higher resistance to fatigue fracture in the in situ irradiation condition than that in the post-irradiation condition was mainly attributed to the delay in the processes of crack initiation and growth until 100 μm in length. Some essential differences of fatigue behaviors between the in situ (dynamic) irradiation and the post-irradiation (static) conditions may be explained in terms of the interaction between the radiation-induced defect clusters and moving dislocations.

References

[1] L.A. James, R.L. Knecht, Nucl. Technol. 19 (1973) 148.
[2] P. Shahinian, ASTM STP 570, ASTM, Philadelphia, PA, 1975, p. 191.
[3] G.J. Lloyd, J.D. Walls, J. Gravenor, J. Nucl. Mater. 110 (1982) 115.
[4] B. Josefsson, U. Bergenlid, J. Nucl. Mater. 212–215 (1994) 525.
[5] R. Scholz, J. Nucl. Mater. 212–215 (1994) 546.
[6] H. Mizubayashi, S. Okuda, K. Nakagome, H. Shibuki, S. Seki, Mater. Trans. Japan. Inst. Met. 25 (1984) 257.
[7] J. Nagakawa, Y. Murase, N. Yamamoto, Y. Fukuzawa, J. Nucl. Mater. 283–287 (2000) 391.
[8] S. Miyazaki, K. Shibata, H. Fujita, Acta Metall. 27 (1979) 855.
[9] Y. Murase, J. Nagakawa, N. Yamamoto, Y. Fukuzawa, ASTM STP 1366, ASTM, West Conshohocken, PA, 2000, p. 713.
[10] T. Yokobori, T. Aizawa, J. Jpn. Inst. Met. 39 (1975) 1003.
[11] W.C. Connors, Mater. Charac. 33 (1994) 245.
[12] M. Gerland, J. Mendez, P. Violan, B. Ait Saadi, Mater. Sci. Eng. A 118 (1989) 83.
[13] Wan-Young Maeng, Mun-Hwan Kim, J. Nucl. Mater. 282 (2000) 32.
[14] S.N. Ghafouri, R.G. Faulkner, T.E. Chung, Mater. Sci. Technol. 2 (1986) 1223.
[15] Y.S. Zheng, Z.G. Wang, S.H. Ai, Mater. Sci. Eng. A 176 (1994) 393.
[16] H.L. Huang, N.J. Ho, W.B. Lin, Mater. Sci. Eng. A 279 (2000) 261.
[17] K. Ehrlich, J. Nucl. Mater. 133&134 (1985) 119.
[18] F.A. Garner, M.L. Hamilton, N.F. Panayotou, G.D. Johnson, J. Nucl. Mater. 103&104 (1981) 803.
[19] R. Tulluri, D.J. Morrison, J. Mater. Eng. Perform. 6 (1997) 454.